Synthesis and Characterization of Poly(ethylene terephthalate) Nanocomposites with Organoclay

Cheng Fang Ou, Mong Ting Ho, Jia Rung Lin

Department of Chemical Engineering, National Chin-Yi Institute of Technology, Taichung 411, Taiwan, Republic of China

Received 22 February 2003; accepted 12 May 2003

ABSTRACT: Poly(ethylene terephthalate) (PET)/montmorillonite (MMT) nanocomposites were prepared by solution intercalation method. The clay was organo-modified with the intercalation agent cetylpyridinium chloride (CPC). Wide-angle X-ray diffraction (XRD) showed that the layers of MMT were intercalated by CPC. Four nanocomposites with organoclay contents of 1, 5, 10, and 15 wt % were prepared by solution blending. XRD showed that the interlayer spacing of organoclay in the nanocomposites depends on the amount of organoclay present. According to the results of differential scanning calorimetry (DSC) analysis, clay behaves as a nucleating agent and enhances the crystallization rate of PET. The maximum enhancement of crystallization rate for the nanocomposites was observed in those containing about 10 wt % organoclay within the studied range of 1–15 wt %. From thermogravimetric analysis (TGA), we found that the thermal stability of the nanocomposites was enhanced by the addition of 1–15 wt % organoclay. These nanocomposites showed high levels of dispersion without agglomeration of particles at low organoclay content (5 wt %). An agglomerated structure did form in the PET matrix at 15 wt % organoclay. © 2003 Wiley Periodicals, Inc. J Appl Polym Sci 91: 140–145, 2004

Key words: nanocomposites; crystallization; clay; nucleation

INTRODUCTION

Poly(ethylene terephthalate) (PET) is a material with low cost and high performance, which has found wide applications in fiber and non-fiber fields. Historically, it has not been considered for applications involving high-speed processing, such as injection molding, because it is a high melting and slow crystallizing polymer. However, crystallization can be increased by the addition of polymeric nucleating agents such as linear low-density polyethylene (LLDPE),[1] poly(methyl methacrylate) (PMMA),[2] poly(phenylene sulfide) (PPS),[3] high-density polyethylene (HDPE),[3] liquid crystalline polymer (LCP),[4–9] and inorganic filler.[10–14] $Al(OH)_3$ is an effective nucleator for PET cooled from the melt, but it is not an effective nucleator for PET crystallization upon heating from the glass.[13] In PET/mica nanocomposites, 4 wt % mica played a strong nucleating role, generating a large increase in the crystallization temperature (T_c), glass transition temperature (T_g) and melting point (T_m) compared to pure PET.[14]

One of the most prevalent classes of composites is composed of materials containing an organic binding matrix with an inorganic material as the reinforcing filler, which comprise one of the most important classes of synthetic engineering materials.[15–17] The incorporation of organic/inorganic hybrids can result in materials possessing high degrees of stiffness, strength, and gas barrier properties with far less inorganic content than is used in conventional filled polymer composites. Layered silicates dispersed as a reinforcing phase in an engineering polymer matrix are among the most important forms of such nanocomposites.

Montmorillonite (MMT) is a filler used in many nanocomposites, such as polyamide/MMT,[18] epoxy/MMT,[19] unsaturated polyester (UP)/MMT,[20] polystyrene (PS)/MMT,[21] and polypropylene (PP)/MMT.[22] Most studies are devoted to the preparation and characterization of new polymer/MMT nanocomposites, including their mechanical, gas permeability, solvent resistance and fire-retarding properties. Very few reports[23–25] have appeared on PET nanocomposites. Ke et al.[23] reported the preparation of a PET/clay nanocomposite, which had three times the crystallization rate of pure PET and showed a heat deflection temperature (HDT) 20–50°C higher than that of pure PET. Davis et al.[25] prepared PET nanocomposites by melt-compounding PET with 5 wt % organically modified MMT (treated with 1,2-dimethyl-3-*N*-hexadecyl imidazolium) under various blending conditions. The composites showed high levels of MMT dispersion and delamination. Processing and incorporation of imidazolium-MMT does not change the inherent thermal stability of PET. Alternative mixing conditions,

Correspondence to: C. F. Ou (oucf@chinyi.ncit.edu.tw).

Journal of Applied Polymer Science, Vol. 91, 140–145 (2004)

longer residence times and higher screw speeds resulted in lower quality nanocomposites. The objectives of this study were to disperse organoclay into a PET matrix and to investigate the effects of organoclay loading on the crystallization behavior and thermal stability of PET/organoclay nanocomposites. In this article, an intercalation agent was used to chemically modify the surface of the pristine clay. We also examined the effect of the concentration of organoclay on the interlayer spacing. These results were analyzed by X-ray diffraction (XRD), differential scanning calorimetry (DSC), thermogravimetric analysis (TGA), and transmission electron microscopy (TEM).

EXPERIMENTAL

Materials

PET resin was kindly donated by the Far East Textile Co (Taoyuan, Taiwan). The resin has an intrinsic viscosity of 0.62 dL/g in 60/40 (w/w) phenol/tetrachloroethane at 30°C. The layered silicate used in this study was a sodium MMT with a cationic exchange capacity (CEC) value of 87 mEq/100g (abbreviated as 8K), which was supplied by Pai-Kong Nano Technology Co Ltd (Taoyuan, Taiwan). The particle size was 0.63 μm. The intercalation agent, cetylpyridinium chloride (CPC), was purchased from Tokyo Chemicals Industry (TCI). Other materials were commercially available and used as received. PET was dried *in vacuo* at 70°C for 48 h prior to solution blending.

Preparation of organoclay and PET/organoclay nanocomposites

A quantity of 5 g of clay was added to 200 mL of distilled water. The dispersion was heated to 60°C with mechanical stirring for 1.5 h. The optimum weight of CPC (CPC/clay = 2/1 by equivalent) was added to the dispersion, and the resultant mixture was stirred at 60°C for 24 h. The solution was filtered and the organoclay was washed thoroughly with 1/9 (w/w) alcohol/H_2O and distilled water three times to remove the residual salt. The organoclay (termed 8K-P) was then dried overnight in a vacuum oven at 70°C.

Nanocomposites were prepared by solution mixing appropriate quantities of finely ground organoclay and PET in the 3/1 (w/w) phenol/chloroform mixed solvent at 60°C for 2 h. Four nanocomposites with organoclay contents of 1, 5, 10, and 15 wt % were prepared for this study. The homogeneous solutions were dried at 80°C in a vacuum for 24 h to remove any remaining solvent and to facilitate complete polymer intercalation between the silicate layers.

X-ray Diffraction

Wide angle XRD experiments were performed on powder specimens using a Shimadzu XD-5 diffractometer with Cu K_α radiation (λ = 0.154056 nm). The generator was operated at 300 kV and 20 mA. Samples were scanned from 2 θ = 2° to 15° at a scanning rate of 2°/min.

DSC measurement

DSC measurements were performed with a TA 2010 analyzer (TA Instruments, New Castle, DE). The sample (≈5–7 mg) was dried at 60°C for 6 h in a vacuum oven before DSC characterization. The temperature and energy readings were calibrated with indium at each measurement. All measurements were carried out in a nitrogen atmosphere. The samples were heated first to 280°C and kept for 3 min in the hermetic cell to remove the thermal history. The sample was then autocooled at 10°C /min to 30°C and reheated at 10°C /min to 280°C. Both crystallization and melting parameters were obtained from cooling and heating scans. T_m was considered to be the maximum of the endothermic melting peak from the heating scans and T_c the maximum of the exothermic peak of crystallization from the cooling scans. The heat of fusion (ΔH_f) and the crystallization heat (ΔH_c) were determined from the areas of the melting peaks and crystallization peaks, respectively, and normalized per gram of PET homopolymer. The results reported are the average of three samples.

Thermogravimetric analysis

The thermal stability of samples was characterized with a DuPont 910 thermogravimetric analyzer. Samples were heated under a nitrogen atmosphere at a heating rate of 10°C /min.

Transmission electron microscopy

TEM photographs of ultrathin sections of the nanocomposites were taken on a Jeol JEM-1200 CXII transmission electron microscope using an acceleration voltage of 120 kV.

RESULTS AND DISCUSSION

Structure of interlayer and dispersibility of organoclay in PET

The XRD patterns of pristine clay (8K), organoclay (8K-P) and nanocomposites containing 1, 5, 10, and 15 wt % 8K-P are presented in Figure 1. For the pristine clay, a peak occurs at approximately 2 θ = 7.21° (d = 1.23 nm), which corresponds to the basal spacing of the (001) plane of clay. The (001) plane peak of the

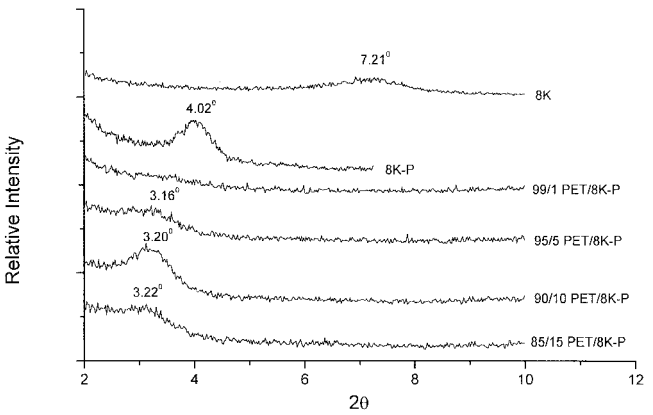

Figure 1 XRD patterns of clay, organoclay, and PET/8K-P nanocomposites.

organoclay is shifted to a lower angle compared to pristine clay. This indicates that intercalation of CPC occurred, and the interlayer spacing of the clay increased. For 8K-P, a large peak at 2 θ = 4.02°, corresponding to interlayer spacing of 2.20 nm, is clearly observed. This reveals that the interlayer spacing of 8K-P increased from 1.23 nm to 2.20 nm.

Intercalation of polymer chains usually increases the interlayer spacing of clay, in comparison with the spacing of the organoclay used, leading to a shift of the diffraction peak toward lower angle values. The (001) plane peaks for the nanocomposites were observed around 3.16-3.22° and shifted to lower angles compared to organoclay 8K-P, except for 1 wt %. In such a nanocomposite, the repetitive multilayer structure is well preserved, allowing the interlayer spacing to be determined. Therefore it can be said that the intercalation of PET chains into the galleries of silicate layers took place. As previously mentioned, the interlayer spacing of 8K-P is 2.20 nm. In 95/5 PET/8K-P, a new and broad peak at 2 θ = 3.16° (d = 2.79 nm) was observed, and the interlayer spacing increased from 2.20 to 2.79 nm. The XRD pattern for 90/10 PET/8K-P has a small shift to a higher diffraction angle compared to 95/5 PET/8K-P. The interlayer spacing decreases from 2.79 nm to 2.76 nm (2 θ = 3.20°) with organoclay loading, from 5 to 10 wt %. The intensity and area of XRD, which at 2 θ = 3.16°, both increase with an increase in the amount of organoclay loading, from 5 to 10 wt %. The peak at 2 θ = 3.22 for 85/15 PET/8K-P is broader than that of 90/10 PET/8K-P but has a small shift to a higher diffraction angle compared to 90/10 PET/8K-P. The diffraction curves of these nanocomposites show an increased tendency in intensity and area at smaller diffraction angles with the content of organoclay. From these results, it can be said that intercalation of PET chains into the galleries of silicate layers occurred, and exfoliation of the organoclay in PET did not. Furthermore, overly large amounts (15 wt %) of organoclay cannot be well dispersed in PET and must exist in the form of an agglomerated layer structure. The variation of interlayer spacing with weight percent of organoclay shows that the different polymer/organoclay weight ratios affect the interlayer spacing of the clay.

The nanocomposite containing 1 wt % 8K-P showed no obvious clay peak around 3.16-3.22° in the XRD pattern. Thus, it might be conjectured that most silicate layers lose their crystallographic ordering in the nanocomposite, and exfoliation of organoclay occurs. However, the lack of peak could be the result of the low concentration of organoclay. In a poly(ethylene terephthalate-*co*-ethylene naphthalate) (PETN)/organoclay nanocomposite,[26] clay particles have been reported to be highly dispersed in the polymer matrix without a large agglomeration of particles at a low clay content (<4 wt %). In our previous report of PET/11K-M (a clay with a CEC value of 114 mEq/100g modified by cetyltrimetylammonium chloride) nanocomposite,[27] according to TEM, the organoclay particles were highly dispersed in the PET matrix without a large agglomeration of particles at low organoclay content (1–5 wt %). However, an agglomerated structure did form in the PET matrix at a 15 wt % organoclay content. In the PET/8K-P nanocomposites, the XRD patterns for 1 and 5 wt % are similar to those of PET/11K-M nanocomposites. These results suggest that both nanocomposites show well dispersed individual clay layers embedded in the polymer matrix, even though a small number of unexfoliated layers still exist.

Effect of organoclay content on crystallization and thermal behavior of PET/organoclay nanocomposites

Figure 2(a) shows the cooling curves of pure PET and PET/8K-P nanocomposites. It is evident that there is a distinct exothermic crystallization peak in all of the cooling scans, and the peak is symmetrical. The DSC thermograms recorded during the cooling of the samples from melt with a constant cooling rate showed a prominent crystallization exothermic peak. When the crystallization exothermic peak is symmetrical, the half crystallization time ($t_{1/2}$) can be obtained from this equation:

$$t_{1/2} = (T_{on} - T_c)/\chi$$

where T_{on} is the crystallization onset temperature, which is the temperature where the thermograph initially departs from the baseline, T_c is the temperature where the exotherm shows a peak, and χ is the cooling rate (°C/min).

The results for $t_{1/2}$ and the thermal dynamics parameters for PET/8K-P nanocomposites are listed in

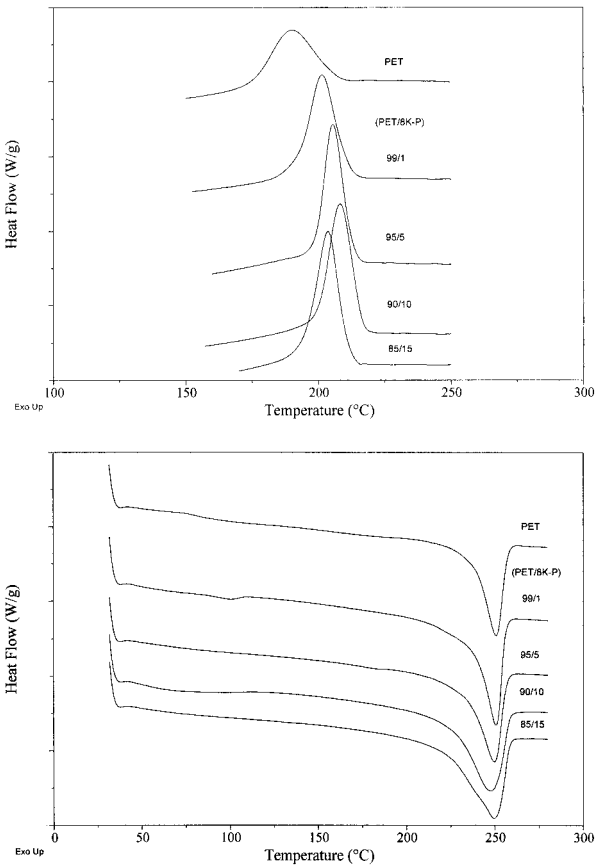

Figure 2 DSC thermograms of neat PET and PET/8K-P nanocomposites: (a) cooling scans, (b) heating scans.

Table I. The crystallization onset temperatures and the T_c values for PET/8K-P nanocomposites are higher than those of pure PET in all four compositions. The 90/10 PET/8K-P exhibits the highest crystallization onset temperature (222°C) and T_c value (208°C) of the PET/8K-P nanocomposites. Changes in the crystallization peak width (ΔT_c) and the heat of crystallization (ΔH_c) are related to the overall crystallization rate and the extent of crystallization, respectively. The ΔT_c values for the blends are narrower by 13 to 16°C than that of pure PET (45°C) and the 90/10 PET/8K-P exhibits the narrowest ΔT_c. The $t_{1/2}$ values of the nanocomposites are smaller than that of pure PET. The 90/10 PET/8K-P exhibits the smallest $t_{1/2}$ (1.45 min), and its crystallization rate is 1.55 times that of pure PET. On the other hand, the values of ΔH_c for all blends are larger than that of PET (38.9 J/g) and increase with increase in the 8K-P content. If the crystallization rate is defined as the heat of crystallization divided by the time from the onset to the completion of crystallization (ΔH_c/time), then the crystallization rates for the PET/8K-P nanocomposites are greater than that of PET (0.144 J g^{-1} s^{-1}). The values of ΔH_c/time increase with the amount of 8K-P organoclay from 1 to 10 wt %, and the 90/10 blend exhibits the greatest value of 0.262 J g^{-1} s^{-1}. In other words, 10 wt % 8K-P accelerates the PET crystallization rate by 1.82 times, while increasing the organoclay content to 15 %, diminishes the value of ΔH_c/time to 0.256 J g^{-1} s^{-1}.

In programmed cooling, the crystallization temperature reflects the overall crystallization rate, attributed to the combined effects of nucleation and growth. Thus the degree of supercooling ($\Delta T = T_m - T_c$) may be a measurement of a polymer's crystallizability; that is, the smaller the ΔT, the higher the overall crystallization rate. The ΔT values for the PET/8K-P nanocomposites are smaller, by 13 to 20°C, than that of pure PET (61°C), and the 90/10 PET/8K-P exhibits the smallest ΔT. The result again reveals that the overall crystallization rate for the PET/8K-P nanocomposites is greater than that of PET.

As shown in Table I, the 90/10 PET/8K-P nanocomposite exhibits the highest crystallization onset temperature and T_c value, the greatest ΔH_c/time (0.262 J g^{-1} s^{-1}), and the smallest ΔT (41°C) among the PET/8K-P nanocomposites. From these results, it can be concluded that 8K-P exhibits a strong heterophase nucleation effect on PET crystallization due to its enormous surface area. The crystallization rate of PET may be accelerated by the addition of 1–15 wt % of 8K-P, where the acceleration efficiency probably reaches a

TABLE I
DSC Data for PET/8K-P Nanocomposites

	Melting[a]				Crystallization[b]						
Composition (PET/8K-P)	Onset (°C)	T_m (°C)	ΔT_m (°C)	ΔH_f (J/g)	T_{on} (°C)	T_c (°C)	ΔT_c (°C)	$t_{1/2}$ (min)	ΔH_c (J/g)	ΔH_c/time (Jg^{-1} s^{-1})	ΔT[c] (°C)
100/0	204	251	55	41.8	212	190	45	2.25	38.9	0.144	61
99/1	204	250	60	50.2	218	202	32	1.60	43.4	0.226	48
95/5	204	250	58	54.5	219	206	29	1.45	44.4	0.255	44
90/10	204	249	60	62.4	222	208	29	1.45	45.5	0.262	41
85/15	203	250	61	68.5	217	204	30	1.50	46.2	0.256	46

[a] From heating scans
[b] From cooling scans
[c] $\Delta T = T_m - T_c$

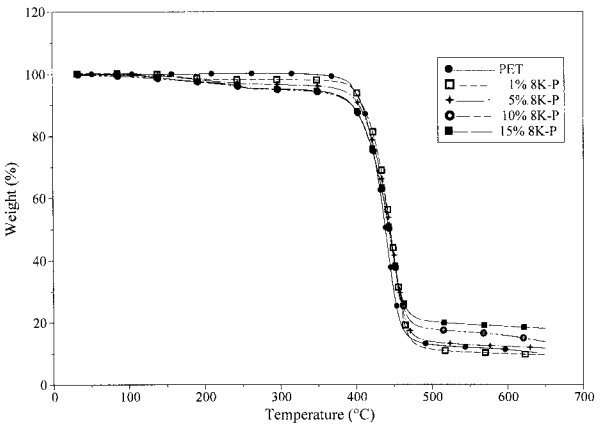

Figure 3 TGA curves of PET/8K-P nanocomposites.

maximum at the 8K-P level of 10 wt %. The result is similar to both systems of nylon1212/MMT[28] and polyamide-6/MMT nanocomposites.[29] In both systems, MMT is an effective nucleating agent due to the high surface area of silicate platelets and their chemical affinity for the polymer, which induce a nucleation and lamellar ordering effect.

Figure 2(b) depicts the heating runs of pure PET and PET/8K-P nanocomposites. There is an endothermic melting peak on all of the heating scans. The various melting parameters determined from heating scans for PET/8K-P nanocomposites are summarized in Table I. The T_m value is virtually unchanged, regardless of organoclay loading. The onset temperatures of melting and melting peak width (ΔT_m) are related to the lowest thermal stability and the distribution of crystallites, respectively. The onset temperature of melting is virtually unchanged, regardless of organoclay loading. A clear increase (3–6°C) in ΔT_m is found in the nanocomposites with respect to neat PET (55°C). In other words, the distribution of crystallites of PET in PET/8K-P nanocomposites is broader than that of neat PET. The values of ΔH_f for all nanocomposites are larger than that of PET (41.8 J/g) and increase with an increase in the 8K-P content. This reveals that the amount (degree) of crystallinity of PET increases with the addition of 8K-P and also with the content of organoclay 8K-P.

Thermal stability

Figure 3 shows the TGA curves of PET/8K-P nanocomposites with different 8K-P contents. The thermal decomposition temperatures (from the differential thermogravimetry (TG) traces, not shown) and the weight percentage of residue at 600°C are listed in Table II. The thermal decomposition temperature (T_d) of neat PET is 435°C. It is observed that the nanocomposites possess higher thermal stability by 4–7°C than neat PET. The thermal decomposition temperatures of the nanocomposites display increases up to 5 wt % organoclay with 95/5 PET/8K-P exhibiting the highest T_d value (442°C). However, increasing the orgaclay content to 15 wt % diminished the T_d value to the extreme low value of 439°C. This increase in the thermal stability of the nanocomposites may result from the barrier effect of the clay layer structure and from the strong interaction between the organoclay and the PET molecules.[30] Furthermore, the clay platelets have a shielding effect on the matrix and slow the rate of mass loss of the decomposition product. For PETN/MMT nanocomposites,[26] a similar trend in thermal stability with increasing MMT (<6 wt %) was observed. In MMT/polyimide (PI) hybrids,[31] thermal stability was found to be higher when MMT (<10 wt %) was well dispersed. As the MMT content increases, the agglomeration tendency of MMT increases, and the thermal stability decreases. The thermal stability of PET/clay nanocomposites showed a 6–19°C increase by the addition of 1.5–5.0 wt % organoclay.[23] The author explains that the nanoscale particles will show a stronger interaction with the PET matrix when the external temperature approaches the degradation temperature. In this study, we concluded that the enhancement of the thermal stability of PET by 1–15 wt % organoclay results from the same phenomenon in the PET/clay nanocomposites.[23] When the clay loading increases to 10–15 wt %, the amount of clay decreases the enhancement of the thermal stability of PET/8K-P nanocomposites. This suggests that the organoclay 8K-P domain can agglomerate above 10 wt % 8K-P content in the PET matrix. This result is consistent with the XRD analysis. These results reveal that the thermal stability of PET/8K-P nanocomposites is related to the organoclay 8K-P content and the dispersion of organoclay in the PET matrix. As seen in Table II, the weight of residue at 600°C increases, ranging from 10.6 to 18.8 wt %, with organoclay loadings of 1–15 wt %. This enhancement of the char formation is ascribed to the high heat resistance exerted by the MMT itself.[32]

Morphology

Figure 4(a, b) shows the TEM photographs of 5 and 15 wt % nanocomposite, respectively. The light gray area

TABLE II
TGA Data for PET/8K-P Nanocomposites

Composition (PET/8K-P)	T_d[a] (°C)	wt_R^{600}[b] (%)
100/0	435	11.3
99/1	441	10.6
95/5	442	12.2
90/10	440	15.6
85/15	439	18.8

[a] Temperature at maximum weight loss rate.
[b] Weight percentage of residue at 600°C.

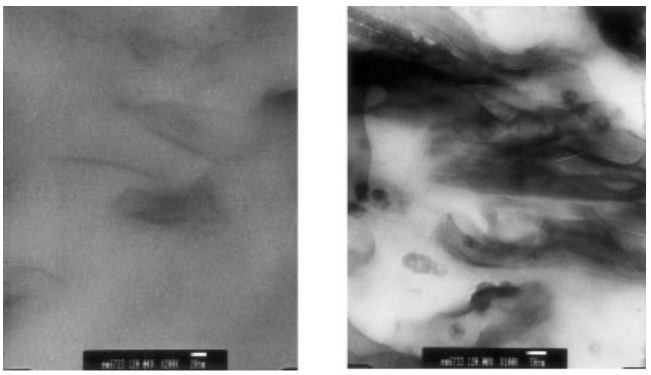

Figure 4 TEM photographs of PET/8K-P nanocomposites containing (a) 5 and (b) 15 wt % 8K-P.

is the PET matrix, and the darker regions are made up of the silicate layers. Both show exfoliated and intercalated systems. TEM of the 5 wt % [Fig. 4(a)] indicates that the organoclay was highly dispersed in the PET matrix, and some of the silicate layers are exfoliated into single layer and randomly dispersed in the polymer matrix, although a number of unexfoliated layers still exist. For the 15 wt % [Fig. 4(b)], the clusters or agglomerated structures form and become denser in the PET matrix.

CONCLUSIONS

PET/8K-P nanocomposites were prepared by solution intercalation. XRD and TEM analysis indicate that intercalated nanocomposites were obtained.

DSC analysis showed PET exhibiting heterogeneous nucleation in the presence of MMT and an increased crystallization rate. MMT is an effective nucleating agent. The 90/10 PET/8K-P exhibits the most significant acceleration of the PET crystallization rate. The nanocomposites with organoclay 8K-P loading from 1–15 wt % exhibit higher thermal stability than pure PET. TEM showed that the 5 and 15 wt % nanocomposites contained both intercalated and exfoliated organoclay layers. The organoclay was highly dispersed in the PET matrix without a large agglomeration of particles in the 5 wt % nanocomposite. However, an agglomerated structure was observed in the 15 wt % nanocomposite.

The authors would like to thank the National Science Council of the Republic of China for financially supporting this research under Contract No. NSC90-2216-E-167-002.

References

1. Bourland, L. Plastics Eng 1987, 39.
2. Nadkarni, V. M.; Jog, J. P. Polym Eng Sci 1987, 27, 451.
3. Nadkarni, V. M.; Shingankuli, V. L.; Jog, J. P. J Appl Polym Sci 1992, 46, 339.
4. Joseph, E. G.; Wilkes, G. L.; Baird, D. G. Prepr Am Chem Soc Div Polym Chem 1983, 24, 304.
5. Sukhadia, A. M.; Done, D.; and Baird, D. G. J Polym Eng Sci 1990, 30(9), 519.
6. Battacharya, S. K.; Tendokar, A.; Misra, A. Mol Cryst Liq Cryst 1987, 153, 501.
7. Sharma, S. K.; Tendokar, A.; Misra, A. Mol Cryst Liq Cryst 1988, 157, 597.
8. Ou, C. F.; Huang, S. L. J Appl Polym Sci 2000, 76, 587.
9. Ou, C. F.; Li, W. C.; Chen, Y. H. J Appl Polym Sci 2002, 86, 1599.
10. Groeninckx, G.; Berghmans, H.; Overbergh, N.; Smets, G. J Polym Sci Polym Phys Ed 1974, 12, 303.
11. Przygocki, W.; Wlochowicz, A. J Appl Polym Sci 1975, 19, 2683.
12. Ibbotson, C.; Sheldon, R. P. Br Polym J 1979, 11, 146.
13. Aharoni, S. M.; Sharma, R. K.; Szobota, J. S.; Vernick, D. A. J Appl Polym Sci 1983, 28, 2177.
14. Saujanya, C.; Imai, Y.; Tateyama, H. Polymer Bull 2002, 49, 69.
15. Messersmith, P. B.; Stupp, S. I. J Mater Res 1992, 7, 2559.
16. Kada, A.; Usuki, A. Mater Sci Eng 1995, C3, 109.
17. Giannelis, E. P. Adv Mater 1996, 8, 29.
18. Agag, T.; Koga, T.; Takeichi, T. Polymer 2001, 42, 3399.
19. Lee, A.; Lichtenhan, J. D. J Polym Sci Polym Chem Ed 1999, 37, 2225.
20. Suh, D. J.; Lim, Y. T.; Lim, O. O. Park, Polymer 2000, 41, 8557.
21. Chen, G.; Liu, S.; Chen, S.; Qi, Z. Macromol Chem and Phys 2001, 202, 1189.
22. Lee, J. W.; Lim, Y. T.; Park, O. O. Polym Bull 2000, 45, 191.
23. Ke, Y.; Long, C.; Qi, Z. J Appl Polym Sci 1999, 71, 1139.
24. Maxfield, M.; Shacklette, L. W.; Baughman, R. H.; Christiani, B. R.; Eberly, D. E. PCT Int APPL WO 93/04118 (1993).
25. Davis, C. H.; Mathias, L. J.; Gilman, J. W.; Schiraldi, D. A.; Shields, J. R.; Trulove, P.; Sutto, T. E.; Delong, H. C. J Polym Sci Polym Phys Ed 2002, 40, 2661.
26. Cheng, J. H.; Park, D. K. J Polym Sci Polym Phys Ed 2001, 39, 2581.
27. Ou, C. F.; Ho, M. T.; Lin J. R. J Polym Res 2003, 10, 127.
28. Wu, Z.; Zhou, C.; Zhu, Na. Polym Testing 2002, 21, 479.
29. Akkapeddi, M. K. Polym Compos 2000, 21, 576.
30. Petrovic, X. S.; Javni, I.; Waddong, A.; Banhegyi, G. J Appl Polym Sci 1999, 3, 2063.
31. Yang, Y.; Zhu, Z. K.; Yin, J.; Wang, X. Y.; Qi, Z. E. Polymer 1999, 40, 4407.
32. Frischer, H. R.; Gielgens, L. H.; Koster, T. P. M. Acta Polym 1999, 50, 122.